Int. J. Solids Structures, 1973, Vol. 9, pp. 981 to 998. Pergamon Press. Printed in Great Britain

A NUMERICAL STUDY OF UNIAXIAL COMPRESSION IN CIRCULAR ELASTIC–PLASTIC COLUMNS

A. NEEDLEMAN

Department of Mathematics, Room 2-337, Massachusetts Institute of Technology, Cambridge, Massachusetts 02139, U.S.A.

Abstract—The boundary value problem for a circular elastic–plastic column in uniaxial compression is posed in two ways. In one, the ends of the column are assumed to be cemented to rigid platens; while in the other they remain shear free. For the latter end condition, one solution corresponding to a state of uniform uniaxial stress is available for all values of applied compression. A class of bifurcation modes from this solution, that includes Euler strut buckling and axisymmetric bulging as special cases, is investigated by means of the finite element method. Here, it is found that the only bifurcation mode likely to be realized in elastic–plastic materials of the class considered here (for realistic values of material parameters) is Euler strut buckling. The entire deformation history of a stubby column cemented to rigid platens is also calculated. In this case, attention is confined to axisymmetric deformations. The results obtained include the overall load–strain curve for the column cemented to rigid platens and the stress and strain distributions at the mid section.

1. INTRODUCTION

THIS paper is concerned with the study of circular elastic–plastic columns under uniaxial compressive loading. Here, the boundary value problem for uniaxial compression is posed in two ways. In both a compressive displacement increment is prescribed at the ends of the column. In one case these ends are required to remain shear free, while in the other the ends are assumed to be cemented to rigid platens.

For the case of shear free ends, one solution, corresponding to a state of uniform uniaxial stress is available for all values of applied compression. A class of bifurcation modes from this solution is considered that includes Euler strut buckling and axisymmetric bulging as special cases. The eigenvalue problem governing bifurcation is posed in terms of a variational principle due to Hill [3, 4], and in this formulation, full account is taken of both geometrical and material non-linearities. Separation of variables is then used in conjunction with the finite element method to obtain a numerical solution to the eigenvalue problem.

A comparison is made between the results obtained here and those of previous workers. For Euler strut buckling, the well known tangent modulus formula was first obtained as the result of a plastic bifurcation analysis by Shanley [1]. Hill and Sewell [2] applied Hill's theory of bifurcation [3, 4] to obtain an approximate solution for the Euler buckling of inelastic columns of arbitrary cross-section built in at one end. Hill and Sewell's [2] result differed from the tangent modulus formula mainly by a shear stiffening term. This term is negligible for sufficiently long columns, the precise specification of "sufficiently long" depending on the properties of the material of which the column is composed as well as on the geometry of the column. Axisymmetric bulging of circular columns was studied by Cheng, Ariaratnam and Dubey [5], for a class of incompressible elastic–plastic

materials, although no numerical results were displayed. Recently, Newman [6] studied the same class of bifurcation modes considered here for rigid-plastic Tresca materials. Surprisingly Newman's results [6] predict that, for stubby columns, the bifurcation stress should be an oscillating function of length to diameter ratio. Furthermore, he found that "higher order" modes had a lower critical stress than either Euler strut buckling or axisymmetric bulging.

For the column cemented to rigid platens, the full boundary value problem must be solved for each increment of applied compression. Here, attention is confined to a stubby column and the deformations are assumed to be axisymmetric. The boundary value problem governing each increment is posed in terms of a variational equation of equilibrium. This variational equation is solved by means of the finite element method and the deformation history is calculated in a linear incremental fashion.

2. BASIC EQUATIONS

For completeness, the basic equations used in the bifurcation and incremental analyses are presented in this section. The formulation given here is identical to that used in a recent study of necking [12], where further details are given. Our approach to the field equations is adopted from [7 and 8].

The volume and surface of a body in an undeformed state are denoted by V and S respectively, and each particle is labelled by a set of convected coordinates x^i $(i = 1, 2, 3)$ which serve as independent variables. In the undeformed body, the covariant components of the metric tensor are given by g_{ij} and its determinant is denoted by g; while in the deformed body these quantities are given by G_{ij} and G respectively.

The Lagrangian strain rate is given by

$$\dot{\eta}_{ij} = \tfrac{1}{2}(\dot{u}_{i,j} + \dot{u}_{j,i} + g_{pq}(\dot{u}^p_{,i}u^q_{,j} + u^p_{,i}\dot{u}^q_{,j})) \tag{1}$$

where u_k are the covariant components of the displacement vector referred to the undeformed base vectors, and $(\ )_{,i}$ denotes covariant differentiation with respect to the undeformed metric tensor. Here, the operation $(\dot{})$ denotes differentiation with respect to some monotonically increasing parameter that characterizes the load history. This parameter is taken to be the magnitude of the compressive displacement at the end of the column, U.

The contravariant components of the Kirchhoff stress tensor on the embedded deformed-coordinates are denoted by q^{ik}. These are related to the contravariant components of the Cauchy stress tensor, $\boldsymbol{\sigma}$, by

$$q^{ik} = (G/g)^{\frac{1}{2}}\sigma^{ik} \tag{2}$$

The stress rates $\dot{q}^{ij}$ are related to the strain rates $\dot{\eta}_{ij}$ by a constitutive relation, to be discussed subsequently, that is of the form

$$\dot{q}^{ij} = L^{ijkl}\dot{\eta}_{kl}. \tag{3}$$

The instantaneous moduli have the symmetries $L^{ijkl} = L^{klij} = L^{lkij} = L^{klji}$ and have two branches, one corresponding to plastic loading and the other to elastic unloading.

The equation of continuing equilibrium may be formulated variationally as follows [3, 4]: among all velocity fields that take on the prescribed velocities on S_u, the actual

velocities satisfy

$$\delta I = 0$$

where

$$I = \frac{1}{2}\int_V [L^{ijkl}\dot{\eta}_{ij}\dot{\eta}_{kl} + q^{ij}g_{pq}\dot{u}^p_{,i}\dot{u}^q_{,j}]\,\mathrm{d}V - \int_{S_T} \dot{T}^i\dot{u}_i\,\mathrm{d}S. \tag{4}$$

Here, $\mathbf{q}$ is the current stress state, $\mathbf{L}$ the corresponding tensor of moduli and $\dot{T}^i$ is given by

$$\dot{T}^i = (\dot{q}^{ik} + \dot{q}^{kj}u^i_{,j} + q^{kj}\dot{u}^i_{,j})n_k. \tag{5}$$

The variational equation of equilibrium (4) serves as the basis for implementing a finite element solution to the axisymmetric compression of a stubby column cemented to rigid platens. An identity, following from the principle of virtual work, that is useful in this incremental calculation, is:

$$\int_V [\dot{q}^{ij}\dot{\eta}_{ij} + q^{ij}g_{pq}\dot{u}^p_{,i}\dot{u}^q_{,j}]\,\mathrm{d}V = \int_S \dot{T}^i\dot{u}_i\,\mathrm{d}S. \tag{6}$$

For the case of a column with shear free ends, one solution, corresponding to a state of uniform uniaxial compression, is available for all values of U. This solution is termed the fundamental solution and is unique for sufficiently small values of U. At some critical compression, say U_c, a bifurcation from the fundamental solution first becomes possible. Then, with the body in a state characterized by a displacement field $\mathbf{u}$ and a stress field $\mathbf{q}$, a non-trivial solution exists to the following set of homogeneous equations:

$$I = \frac{1}{2}\int_V [\dot{q}^{*ij}\dot{\eta}^*_{ij} + q^{ij}g_{pq}\dot{u}^{*p}_{,i}\dot{u}^{*q}_{,j}] = 0 \tag{7a}$$

$$\delta I = 0 \tag{7b}$$

$$\dot{u}^*_i = 0 \quad \text{on} \quad S_u. \tag{7c}$$

Here, the superscript * denotes the difference between field quantities associated with the fundamental solution and those associated with the second solution, and the strain rates $\dot{\eta}^*_{ij}$ are related to the velocities by (1). This result, in its full generality, is due to Hill [3, 4].

If the increment in the fundamental solution at U_c has the property that loading occurs everywhere in the current plastic zone, the stress rates in (7a) are related to the strain rates by

$$\dot{q}^{*ij} = L^{ijkl}\dot{\eta}^*_{kl}. \tag{7d}$$

Furthermore, the branch of the tensor of moduli for plastic loading is to be used in (7d). Thus, the system of equations (7) is independent of the loading–unloading criterion; and in Hill's [3, 4] terminology a linear comparison solid has been introduced.

Although no attempt is made here to study the post-bifurcation behavior of the column, we note that the amplitude of the bifurcation mode is uniquely determined by the requirement that loading occurs everywhere in the current plastic zone, except at one point or along one curve where neutral loading takes place [9].

The particular stress–strain law used in this study is of the form (3) and is a large-strain generalization of J_2-flow theory with isotropic hardening, due to Budiansky [10].

It is assumed that the total strain rate can be written as the sum of the elastic strain rate, $\dot{\eta}^e_{ij}$, and the plastic strain rate, $\dot{\eta}^p_{ij}$. The elastic strain-rate stress-rate relation is taken to be

$$\dot{\eta}^e_{ij} = \frac{1}{E}[\tfrac{1}{2}(1+\nu)(G_{ik}\dot{\sigma}^k_j + G_{jk}\dot{\sigma}^k_i) - \nu G_{ij}\dot{\sigma}^k_k]. \tag{8}$$

Here, σ^i_j are mixed components of Cauchy stress, ν is Poisson's ratio, and E is Young's modulus. This relation does not admit a potential in the large strain region, but when linearized it does give Hooke's law. Since this stress–strain law is intended to apply to situations in which the elastic strains remain small, it is expected that the use of (8) instead of a truly elastic relation will not result in significant error in the total strain. The yield function for J_2-flow theory with isotropic hardening is $F = \sigma_e - c$, where c is either the maximum value of σ_e over the stress history or the initial yield stress σ_y, whichever is greater and σ_e is given by

$$\sigma_e = [\tfrac{3}{2}G_{ik}G_{jl}S^{ij}S^{kl}]^{\frac{1}{2}} \tag{9}$$

where

$$S^{ij} = \sigma^{ij} - \tfrac{1}{3}G^{ij}G_{kl}\sigma^{kl}. \tag{10}$$

The generalized flow rule takes the form

$$\dot{\eta}^p_{ij} = \begin{cases} \dfrac{3}{2}\left(\dfrac{1}{E_t} - \dfrac{1}{E}\right)S_{ij}\dfrac{\dot{\sigma}_e}{\sigma_e} & \text{if } \sigma_e = c \text{ and } \dot{\sigma}_e \geq 0 \\ 0 & \begin{cases} \text{if (i) } \sigma_e < c \\ \text{or (ii) } \sigma_e = c \text{ and } \dot{\sigma}_e \leq 0. \end{cases} \end{cases} \tag{11}$$

Here, E_t is a function of the stress invariant σ_e and is the slope of the true-stress natural strain curve in uniaxial tension.

The constitutive equations may be inverted to find the stress rates in terms of the strain rates (as has been done by Chen [11]) to obtain

$$\dot{\sigma}^{ij} = \left\{\frac{1}{\varepsilon_y(1+\nu)}G^{ik}G^{jl} + \frac{\nu}{\varepsilon_y(1+\nu)(1-2\nu)}G^{ij}G^{kl} - \sigma^{ik}G^{jl} - \sigma^{jk}G^{il} - \frac{3\Lambda S^{ij}S^{kl}}{2\varepsilon_y(1+\nu)\sigma_e^2}\frac{[E/E_t - 1]}{[\frac{2}{3}(1+\nu) + E/E_t - 1]}\right\}\dot{\eta}_{kl}. \tag{12}$$†

Here,

$$\Lambda = \begin{cases} 0 & \text{if (i) } \sigma_e < c \text{ or (ii) } \sigma_e = c \quad \text{and} \quad S_{ij}\dot{\eta}_{ij} \leq 0 \\ 1 & \text{if } \sigma_e = c \quad \text{and} \quad S^{ij}\dot{\eta}_{ij} \geq 0 \end{cases} \tag{13}$$

and

$$\varepsilon_y = \frac{\sigma_y}{E}. \tag{14}$$

The contravariant components of Kirchhoff stress q_{ij} differ from the contravariant components of Cauchy stress by a factor $(G/g)^{\frac{1}{2}}$. This factor is equal to the change in

† In (12) and subsequently all stress quantities are non-dimensionalized with respect to the yield stress, σ_y.

volume between the deformed and undeformed configurations. Since the plastic strain increments given by (11) are incompressible, the volume change is due entirely to the elastic strains which are assumed to remain small. Hence, the approximation $\sigma^{ij} \simeq q^{ij}$ will involve little error and σ^{ij} will be replaced by q^{ij} in the constitutive equation (12).

An alternative derivation of the constitutive relation could proceed by replacing the Cauchy stress components appearing in (8–11) with the corresponding Kirchhoff stress components. In this derivation, however, the tangent modulus, E_t, would differ slightly from the slope of the true-stress natural-strain curve.

In the present study, two representations of uniaxial stress–strain behavior are used. One is the Ramberg–Osgood relation given by

$$\left(\frac{\varepsilon}{\varepsilon_y}\right) = \left(\frac{\sigma}{\sigma_y}\right) + \alpha\left(\frac{\sigma}{\sigma_y}\right)^n. \tag{15}$$

The other is a piece-wise power law of the form

$$\left(\frac{\varepsilon}{\varepsilon_y}\right) = \begin{cases} \left(\dfrac{\sigma}{\sigma_y}\right) & \sigma \leq \sigma_y \\ \left(\dfrac{\sigma}{\sigma_y}\right)^n & \sigma \geq \sigma_y. \end{cases} \tag{16}$$

Here, ε is the natural strain, σ is the true stress, and n is the strain hardening exponent. The Ramberg–Osgood relation is more convenient to use in Euler buckling calculations since it exhibits a continuous tangent modulus, whereas the piece-wise power law is more convenient in the incremental calculation as it gives rise to a sharp yield point.

In the Ramberg–Osgood relation (15), $\sigma = \sigma_y$ implies that $\varepsilon = (1+\alpha)\varepsilon_y$, so that σ_y is a reasonable approximation to the yield stress only if α is small. In this paper, α will always be taken to be 0·1.

3. BIFURCATION ANALYSIS

The circular column studied here has initial length $2L_0$ and initial radius R_0. Cylindrical coordinates are used with $x^1 = r$, $x^2 = \theta$ and $x^3 = z$.

The column is compressed parallel to the z-axis, while the ends remain shear free. Also, the lateral surfaces are required to remain traction free. Thus, the boundary conditions are

$$\dot{T}^1(r, \theta, \pm L_0) = \dot{T}^2(r, \theta, \pm L_0) = 0 \tag{17a}$$

$$\dot{u}_3(r, \theta, \pm L_0) = \pm \dot{U} \tag{17b}$$

$$\dot{T}^i(R_0, \theta, z) = 0 \qquad i = 1, 2, 3. \tag{17c}$$

The fundamental solution is given by

$$\begin{aligned} u_z &= -\left(\frac{U}{L_0}\right)z \\ u_\theta &= 0 \\ u_r &= br \end{aligned} \tag{18}$$

where

$$b = \begin{cases} \exp\left[\varepsilon_y\left(v\sigma + \frac{\alpha}{2}\sigma^n\right)\right] - 1 & \text{(19a)} \\ \exp\left[\varepsilon_y\left(v\sigma + \frac{1}{2}\left(\sigma^n - \sigma 1\right)\right)\right] - 1 \qquad \sigma \geq 1 & \text{(19b)} \end{cases}$$

and

$$\tilde{a} = \left(\frac{U}{L_0}\right) = \begin{cases} -\exp[-\varepsilon_y(\sigma + \alpha\sigma^n)] + 1 & \text{(20a)} \\ -\exp[-\varepsilon_y\sigma^n] + 1 \qquad \sigma \geq 1. & \text{(20b)} \end{cases}$$

Here, (19a and 20a) are the fundamental solution for the Ramberg–Osgood representation of unixial stress-strain behavior while (19b and 20b) are the fundamental solution for the piecewise power law.

Now, we seek a bifurcation of the form

$$\begin{aligned} \dot{u}_r^* &= v_r(r)\cos k\theta \sin\left(\frac{\pi z}{2L_0}\right) \\ \dot{u}_\theta^* &= rv_\theta(r)\sin k\theta \sin\left(\frac{\pi z}{2L_0}\right) \\ \dot{u}_z^* &= v_z(r)\cos k\theta \cos\left(\frac{\pi z}{2L_0}\right). \end{aligned} \tag{21}$$

This assumed bifurcation mode satisfies both the shear free end condition (17a) and the homogeneous velocity condition (7c) identically. When (21) is substituted into the bifurcation functional (7a) and the integrations with respect to θ and z are performed, (7) reduces to

$$\begin{aligned} I = \int_0^{R_0} \Bigg\{ & c_1\left[v_r'^2 + \left(\frac{v_r + kv_\theta}{r}\right)^2\right] + c_2 v_z^2 + 2c_3 v_r'\left(\frac{v_r + kv_\theta}{r}\right) - 2c_4 v_z\left[v_r' + \frac{v_r + kv_\theta}{r}\right] \\ & + c_5\left[v_\theta' - \left(\frac{v_\theta + kv_r}{r}\right)\right]^2 + c_6\left[\left(\frac{\pi}{2L_0}\right)(1+b)v_r + (1+a)v_z'\right]^2 \\ & + c_6\left[\left(\frac{\pi}{2L_0}\right)(1+b)v - (1+a)k\frac{v_z}{r}\right]^2 - \left(\frac{\pi}{2L_0}\right)^2 \frac{\sigma_c}{(1+a)^2}(v_r^2 + v^2 + v_z^2)\Bigg\} r\,dr = 0 \end{aligned} \tag{22a}$$

$$\delta I = 0. \tag{22b}$$

Here, $(\ )'$ denotes d/dr and the constants c_1 $(i = 1, 6)$ depend on σ_c, the effective stress at bifurcation, and are determined from the constitutive equation (12).

The variational equations (22) will be used to determine an approximate critical stress, σ_c, and an approximate eigenmode. The advantage of this formulation is that the trial functions of the variational method need only satisfy the essential boundary conditions of the problem. The natural boundary conditions are then satisfied approximately by the solution of (22).

In the present problem, the essential boundary conditions depend on the azimuthal wave number, k, and follow directly from the requirement that (22a) be finite. For $k = 0$,

axisymmetric bulging, the only essential boundary condition is

$$v_r(0) = 0. \tag{23}$$

While for the shear free conditions employed here it is possible for an axisymmetric bulge to appear at one of the platens, we expect bulging to occur symmetrically about the mid-plane of the column. Thus, for convenience, in the case of axisymmetric bulging, $2L_0$ will be identified as the half-length of the column, will be denoted by L_H, and we will assume the axisymmetric mode is symmetric about the mid-plane of the column.

For azimuthal wave number $k = 1$, the essential boundary conditions are

$$v_r(0) + v_\theta(0) = 0 \tag{24a}$$

$$v_z(0) = 0. \tag{24b}$$

Here, (24a) is equivalent to the requirement that $G^{22}\dot{\eta}^*_{22}$ be finite at $r = 0$. The essential boundary conditions (24) apply to the bifurcation mode that is termed Euler strut buckling.

For $k > 1$, the essential boundary conditions are

$$v_r(0) = v_\theta(0) = v_z(0) = 0. \tag{25}$$

The condition that both $v_r(0)$ and $v_\theta(0)$ vanish arises from the requirement that the terms in (22a) involving $(v_r + kv_\theta)^2$ and $(v_\theta + kv_r)^2$ vanish at $r = 0$. Thus, it is only possible for the centerline of the column to deflect with $k = 1$ in the Euler buckling mode (24). However, it is certainly possible to impose (25) for $k = 1$, although such a mode would have a bifurcation stress no less than the mode with essential boundary conditions (24). Here, for comparison purposes, we will admit the possibility of a bifurcation mode with $k = 1$, satisfying (25).

The numerical method used to implement a solution to (22) is based on the finite element method and is essentially the same as that used in a previous study of necking [12]. The interval $[0, R_0]$ is divided into sub-intervals of length $h = R_0/(j-1)$ where j is the number of nodal points. The functions v_r, v_θ and v_z are taken to be linear in r in each sub-interval.

To begin the bifurcation calculation, an initial guess is made for the critical stress, σ_c, and the corresponding instantaneous stiffness matrix is computed. The variational equation (22b) becomes

$$\mathbf{A}(\sigma_c)\mathbf{x} = 0 \tag{26}$$

where the symmetric matrix $\mathbf{A}$ is the assembled stiffness matrix after the appropriate essential boundary conditions (23, 24 or 25) have been imposed and $\mathbf{x}$ is the vector of nodal velocities.

Cholesky decomposition is used to factor $\mathbf{A}$ into

$$\mathbf{A} = \mathbf{M}^T\mathbf{M} \tag{27}$$

where $\mathbf{M}$ is a lower triangular matrix and $\mathbf{M}^T$ its transpose. Now,

$$\det \mathbf{A} = (\det \mathbf{M})^2 \tag{28}$$

and since $\det \mathbf{M}$ is the product of its diagonal entries, $\det \mathbf{A}$ vanishes when one of these diagonal entries, say M_{ii}, is zero. A Newton–Raphson type iteration was used to determine the smallest value of σ_c for which $\det \mathbf{M} = 0$. Then, by deleting the ith equation and setting the nodal velocity x_i equal to unity, the bifurcation mode is calculated.

Finally, for the case of axisymmetric bulging, $k = 0$, and elastic incompressibility, $\nu = \frac{1}{2}$, an explicit analytical bifurcation criterion may be obtained as has been done by Cheng, Ariaratnam and Dubey [5].

The case of strict material incompressibility requires a slight modification of the bifurcation analysis, since a hydrostatic pressure must now be introduced. However, this calculation parallels that in [5] and only the final result will be given here. The bifurcation condition is

$$(1-q_1^2)J_1(mq_1)[f_1J_1(mq_2)-mq_2J_0(mq_2)(f_2+q_2^2)]$$
$$= (1-q_2^2)J_1(mq_2)[f_1J_1(mq_1)-mq_1J_0(mq_1)(f_2+q_1^2)]. \tag{29}$$

Here, $J_0(\ )$ and $J_1(\ )$ are Bessel functions of the first kind of order zero and one respectively and

$$m = \left(\frac{\pi R_0}{L_H}\right)\frac{1+b}{1+a} \tag{30}$$

$$q_1 = (2-3\psi)^{-\frac{1}{2}}[(1-3\phi)+i(4-9\psi^2-(1-3\phi)^2)^{\frac{1}{2}}]^{\frac{1}{2}} \tag{31a}$$

$$q_2 = (2-3\psi)^{-\frac{1}{2}}[(1-3\phi)-i(4-9\psi^2-(1-3\phi)^2)^{\frac{1}{2}}]^{\frac{1}{2}} \tag{31b}$$

$$f_1 = \frac{4}{2-3\psi} \tag{31c}$$

$$f_2 = \frac{6\phi-3\psi}{2-3\psi} \tag{31d}$$

$$\phi = \frac{E_t}{E} \tag{32a}$$

$$\psi = \frac{\sigma_c}{E} \tag{32b}$$

where $i = (-1)^{\frac{1}{2}}$, a and b are determined by (19 and 20) with $\nu = \frac{1}{2}$, and L_H is the half-length of the column.

4. BIFURCATION RESULTS

The main result of the bifurcation calculations is that the only bifurcation mode likely to be realized in elastic–plastic materials of the class considered here (for realistic values of material parameters), is Euler column buckling. Other modes are probably available but they require such enormous compressive strains to be activated that it is doubtful they could be experimentally achieved.

In Fig. 1, the bifurcation stress for Euler buckling is shown for a Ramberg–Osgood material with $n = 8$, $\varepsilon_y = 0{\cdot}0072$, $\nu = \frac{1}{3}$, $\alpha = 0{\cdot}1$. Also shown in this figure are curves obtained from two approximations; one is the Rayleigh–Ritz approximation of Hill and Sewell [2]. Here, specialized to the case of a circular column with shear free ends, the

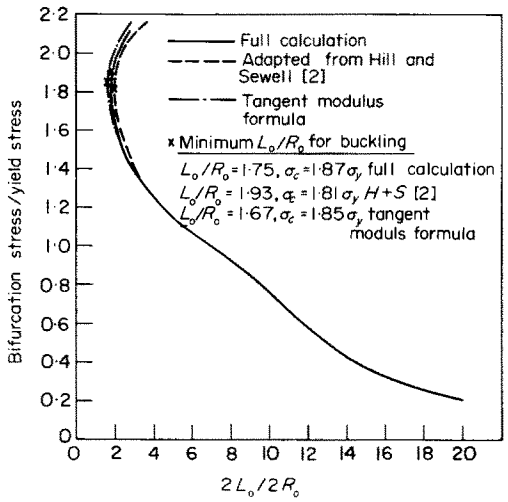

FIG. 1. Curve of critical stress vs length to diameter ratio for Euler buckling (Ramberg–Osgood material with $n = 8$, $\varepsilon_y = 0{\cdot}0072$, $\nu = \frac{1}{3}$, $\alpha = 0{\cdot}1$).

approximate velocity field is given by

$$v_r = \frac{-1}{(1+b)} + \frac{1}{2}\left(\frac{\pi}{2L_0}\right)^2 \frac{(1+b)}{(1+a)^2}\beta r^2 \tag{33a}$$

$$v_\theta = \frac{1}{(1+b)} + \frac{1}{2}\left(\frac{\pi}{2L_0}\right)^2 \frac{(1+b)}{(1+a)^2}\beta r^2 \tag{33b}$$

$$v_z = \left(\frac{\pi}{2L_0}\right)\frac{1}{(1+a)} r \tag{33c}$$

where a and b are determined from (19 and 20) and β is given by

$$\beta = \tfrac{1}{2} + (\nu - \tfrac{1}{2})\frac{E_t}{E}. \tag{34}$$

When (33) is substituted into the bifurcation functional (22a), the following approximation is obtained for the bifurcation stress, σ_c.

$$\sigma_c\left[1 + \frac{1}{4}\left(\frac{\pi R_0}{2L_0}\right)^2\left(\frac{1+b}{1+a}\right)^2 + \frac{1}{24}\beta^2\left(\frac{\pi R_0}{2L_0}\right)^4\left(\frac{1+b}{1+a}\right)^4\right]$$
$$= \frac{1}{4}\left(\frac{\pi R_0}{2L_0}\right)^2\left(\frac{1+b}{1+a}\right)^2(E_t + 2\sigma_c) + \frac{1}{24}\left(\frac{E}{1+\nu} + \sigma_c\right)\beta^2\left(\frac{\pi R_0}{2L_0}\right)^4\left(\frac{1+b}{1+a}\right)^4 \tag{35}$$

The tangent modulus formula is obtained by neglecting the shear stiffening term on the right hand side of (35) and by neglecting both terms on the left side of (35) involving the ratio $(\pi R_0/2L_0)$.

For length to diameter ratios greater than 3, the full numerical solution, the Ritz approximation (35), and the tangent modulus formula all agree within 1 per cent. For

more stubby columns the difference is greater, but all give qualitatively similar results. In particular all predict a minimum length to diameter ratio at which Euler buckling is possible. Actually, for stubby columns, the tangent modulus formula is slightly closer to the numerical solution than the Ritz approximation. *We note that although this is true for a circular column with the material parameters used here, it may not be true for columns with other cross-section shapes or other values of the material parameters.*

As expected, the critical stresses (obtained by the full numerical calculation) did not depend very much on Poisson's ratio, ν. Here, it was found that for $n = 8$, $\varepsilon_y = 0{\cdot}0072$, $\alpha = 0{\cdot}1$, $L_0/R_0 = 6$, varying ν between $\frac{1}{3}$ and 0·48 altered σ_c by less than 0·1 per cent.

In most cases, 21 points ($\Delta r = 0{\cdot}05$) were used in the calculations performed to obtain Fig. 1. For certain values of L_0/R_0, these eigenvalue calculations were repeated with 11 points ($\Delta r = 0{\cdot}1$) and 41 points ($\Delta r = 0{\cdot}025$). The bifurcation stresses obtained with 11 points agreed with those obtained with 41 points to at least three significant figures.

We note that a slight modification of the iteration procedure described in Section 3 was needed to obtain the upper portion of the curve in Fig. 1. Here, the bifurcation stress σ_c was fixed and the iteration was performed on (L_0/R_0).

For $n = 8$, $\varepsilon_y = 0{\cdot}0072$, $\alpha = 0{\cdot}1$, $\nu = \frac{1}{3}$, a numerical search revealed no other mode with a critical compressive strain U/L_0 less than 0·99. It was not possible to determine whether or not bifurcation occurs in the range $1 \geq U/L_0 > 0{\cdot}99$, because computation for such large compressions is extremely difficult.

The unsuccessful search for axisymmetric and higher order modes was conducted as follows. At several values of $L_0/R_0 > 1{\cdot}75$ m a search was made for a mode with a bifurcation stress less than that for Euler strut buckling and none was found. For $L_0/R_0 < 1{\cdot}75$ an extensive search was made for any mode with a critical compressive strain U/L_0, less than 0·99. A computer program was written to evaluate the analytical bifurcation criterion (29) in which $\nu = \frac{1}{2}$. The criterion (29) was evaluated for values of U/L_0 up to 0·99 and no bifurcation was found. Also, the finite element program based on (22) revealed no axisymmetric or higher order modes with a critical compressive strain, U/L_0, less than 0·99. These finite element calculations were performed with 501 points ($\Delta r = 0{\cdot}002$). Thus, our results indicate that for $n = 8$, $\varepsilon_y = 0{\cdot}0072$ and $L_0/R_0 < 1{\cdot}75$, the height of the column can be reduced to $\frac{1}{100}$ of its original value, without bifurcating from the fundamental solution.

The conclusion that stubby columns of structural metals do not bifurcate is not without some experimental support. Phillips [13] has reported unpublished experimental work by Jovane at the National Engineering Laboratory, East Kilbride, in which homogeneous compressive strains of up to 0·99 were achieved in structural metals by carefully lubricating the specimen-platen interface. However, Phillips [13] did not report the original length to diameter ratio (L_0/R_0) of the specimens used.

For an *unrealistically high rate of hardening* ($n = 2$), bifurcation results were obtained for a variety of modes. These results are displayed in Table 1. Note that reductions in height of more than 92 per cent are required for bifurcation. The critical stress obtained for axisymmetric bulging from (29), in which $\nu = \frac{1}{2}$, was $56{\cdot}71\sigma_y$. This differs by about 1·5 per cent from the result in Table 1, where $\nu = \frac{1}{3}$.

Figure 2 shows the bifurcation mode obtained for axisymmetric bulging ($k = 0$). Nearly all the deformation is confined to a small region near the lateral surface of the column. This is also characteristic of the modes obtained for the higher values of azimuthal wave number, k. Although, of course, these modes involve v_θ as well as v_r and v_z. The mode

TABLE 1. BIFURCATION STRESSES FOR $n = 2$, $\varepsilon_y = 0{\cdot}0072$, $\nu = \frac{1}{3}$, $\alpha = 0{\cdot}1$

Azimuthal wave No. k	Column dimensions	Bifurcation stress / Yield stress (σ_c)	Compressive strain at $(U/L_0)_c$ bifurcation
0	$L_H/R_0 = 1$	56·01	−0·9300
1†	$L_0/R_0 = 1$	55·49	−0·9268
1	$L_0/R_0 = 1$	55·49	−0·9268
2	$L_0/R_0 = 1$	55·53	−0·9271
4	$L_0/R_0 = 1$	55·70	−0·9281
6	$L_0/R_0 = 1$	55·96	−0·9298
9	$L_0/R_0 = 1$	56·45	−0·9327
14	$L_0/R_0 = 1$	57·34	−0·9379

† Euler column buckling.

in Fig. 2 is similar to that obtained by Vaughan [14] for axisymmetric bulging of elastic solids.

As can be seen in Table 1, both modes with azimuthal wave number, k, equal to unity have approximately the same bifurcation stress. This is because the Euler buckling mode is nearly the same as that obtained from the mode corresponding to the boundary conditions (25), in fact for Euler buckling

$$v_r(0) = -v_\theta(0) \simeq -6 \times 10^{-13} \times v_z(R_0). \tag{36}$$

This indicates that the curve of critical stress versus length to diameter ratio, L_0/R_0, is qualitatively different for $n = 2$ from the corresponding curve for $n = 8$. For the case $n = 2$, as L_0/R_0 decreases, $v_r(0)$ and $v_\theta(0)$ obtained from the bifurcation mode for Euler buckling decrease until they almost vanish and the two modes with $k = 1$ become nearly identical. On the other hand, for $n = 8$ the curve begins to bend back at $L_0/R_0 = 1{\cdot}75$, $\sigma_c = 1{\cdot}87$. At this point

$$v_r(0) = -v_\theta(0) = -0{\cdot}98 \times v_z(R_0). \tag{37}$$

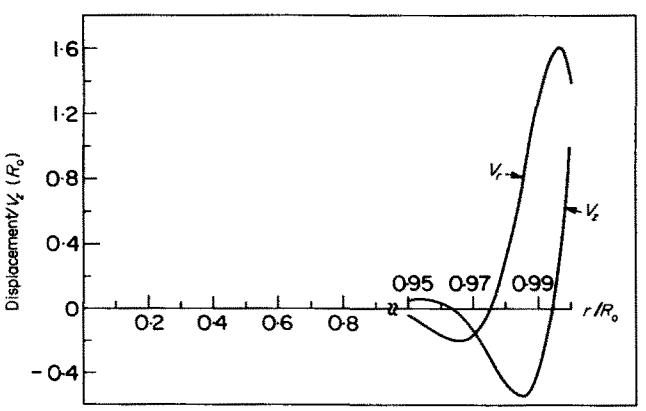

FIG. 2. Axisymmetric eigenmode for $n = 2$, $\varepsilon_y = 0{\cdot}0072$, $\nu = \frac{1}{3}$, $\alpha = 0{\cdot}1$, $L_H/R_0 = 1$.

Also, the results in Table 1 show that the critical stress for $k = 0$ is greater than that for $k = 1$, but for $k > 1$ the critical stress is a slowly increasing function of azimuthal wave number k.

We note that these calculations required far more points than were required for Euler strut buckling. Most of the results displayed in Table 1 were obtained with 501 points ($\Delta r = 0{\cdot}002$). A few calculations were repeated with 651 points ($\Delta r = 0{\cdot}00154$) and the critical stresses obtained in these calculations were within 0·8 per cent of the values obtained with 501 points.

As stated in the Introduction, the results obtained here are quite different from those obtained by Newman [6]. Newman's formulation of the problem was different from that employed here and he considered rigid plastic Tresca type materials. For long columns, Newman's results [6] for Euler strut buckling were in fairly close agreement with the tangent modulus formula, but for stubby columns he found that the critical stress was an oscillating function of L_0/R_0. Also, for long columns, Newman [6] found that there were higher order modes with critical stresses less than the critical stress for Euler buckling.

5. RESULTS FOR A STUBBY COLUMN CEMENTED TO RIGID PLATENS

In this section, the results of an incremental calculation of the deformation history of a stubby column will be presented. The column is of initial length $2L_H$ and initial radius R_0. Here, only axisymmetric deformations will be considered, and, in addition, it is assumed that the deformations are symmetric about the midplane $z = 0$. We imagine the column to be cemented to rigid platens so that at $z = L_H$, the boundary conditions are

$$\dot{u}_1(r, L_H) = 0 \qquad \dot{u}_3(r, L_H) = -\dot{U}. \tag{38}$$

Subsequently (38) will be referred to as the cemented end condition.

In this calculation the piece-wise power law model of uniaxial stress strain behavior is employed with the following set of material parameters:

$$n = 8 \qquad \varepsilon_y = 0{\cdot}0072 \qquad \nu = \tfrac{1}{3}, \tag{39}$$

also, the ratio L_H/R_0 is taken to be one.

A numerical solution to the incremental equilibrium equation (6) is obtained by means of the finite element method. The computer program used to implement this solution is identical to that employed in a recent study of necking [12] except, of course, that here a negative displacement increment is applied at $z = L_H$. Since a description of the numerical procedure is given in [12], only some of the features of the calculation will be described here. Further details are given in [12].

1. A grid with 613 nodal points was used, arrayed as shown in Fig. 3 with $\Delta r = \Delta z = \frac{1}{17}$, and the displacement increments are taken to be linear in r and z in each element.

2. The load increment is calculated from the identity (6), instead of by extrapolation of element stresses to the boundary.

3. Loading or unloading in each element is determined as follows: if the stress state of an element is on its current yield surface, the loading branch of the moduli are taken to be active. If σ_e for that element turns out to be negative, elastic unloading takes place in the next increment. This procedure is only accurate if small increments are used and the

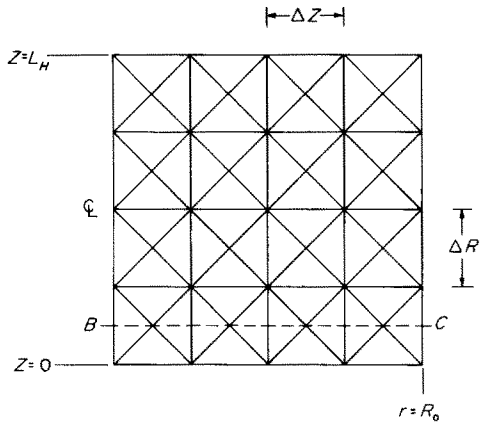

FIG. 3. Coarse version of finite element grid.

transition from loading to unloading (or vice versa) in any element occurs smoothly and only once or twice during the loading history.

The curve of load versus engineering strain is shown in Fig. 4. For comparison purposes, the curve obtained from (19b and 20b) for the case of shear free ends is also shown. It can be seen that the curve for the cemented end condition has a higher apparent yield stress, even though local plastic deformation has taken place at loads below σ_y. At large strains ($U/L_H > 0{\cdot}075$), the curves are nearly parallel, indicating that, although the cemented column is "stiffer" than the column with shear free ends, the apparent rate of hardening is nearly independent of the boundary conditions.

The radial displacement at the mid-section ($z = 0$) is shown in Fig. 5 for both sets of end conditions. As expected, the radial displacement at $z = 0$ is greater for the column

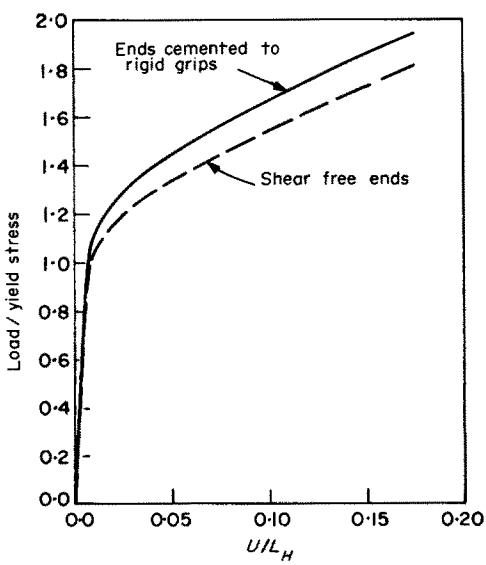

FIG. 4. Curves of load vs compressive strain ($n = 8$, $\varepsilon_y = 0{\cdot}0072$, $\nu = \frac{1}{3}$, $L_H/R_0 = 1$).

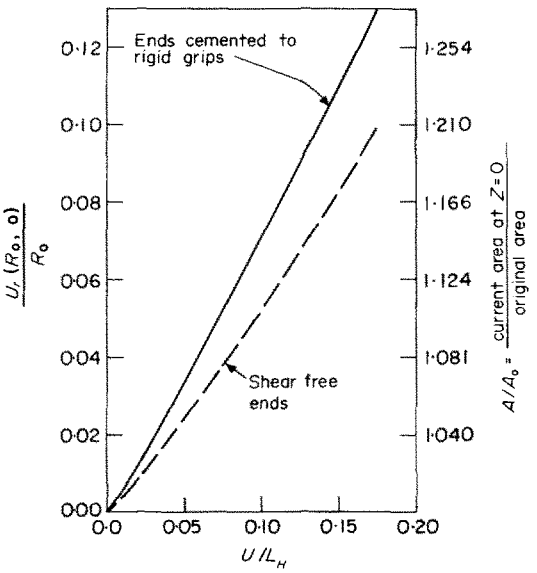

FIG. 5. Curves of radial displacement at midsection vs compressive strain ($n = 8$, $\varepsilon_y = 0{\cdot}0072$, $\nu = \frac{1}{3}$, $L_H/R_0 = 1$).

with cemented ends, which "bulges" out, than for the column with shear free ends, that expands uniformly.

In Fig. 6, the current plastic zone and deformed shape of the column with cemented ends is shown at various stages of compression. The plastic zones displayed here were

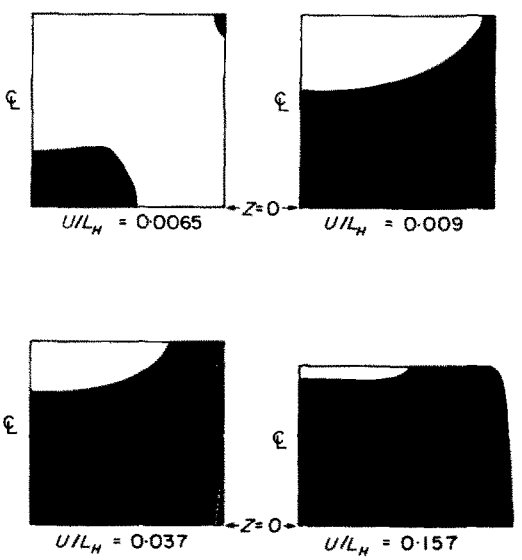

FIG. 6. Development of plastic zone (shaded area) and deformed configuration for stubby column cemented to rigid grips ($n = 8$, $\varepsilon_y = 0{\cdot}0072$, $\nu = \frac{1}{3}$, $L_H/R_0 = 1$).

obtained by sketching smooth curves through the elements on the elastic plastic boundary. Plastic deformation begins in a small region near the lateral surface of the column at the cemented end. Then, a large region of plastic deformation appears near the axis of the column along the midsection $z = 0$. This region grows and finally links up to the small region at the lateral surface of the column. Hereafter, the plastic zone grows slowly and even at the last stage shown ($U/L_H = 0{\cdot}157$) there is a region that has not yet yielded. It can also be seen from this figure that the bulge that develops is not very pronounced.

Next, Fig. 7 shows sketches of contours of constant effective stress, in the original configuration, at two stages of compression. In the early stage of compression, $U/L_H = 0{\cdot}009$, the regions of high effective stress are confined to the corners $z = 0$, $r = 0$ and $z = L_H$, $r = R_0$. At $z = L_H$, $r = R_0$ the stresses are singular, but as can be seen in this figure the high stresses due to the singularity are confined to the elements bordering this corner. However, at the latter stage a diagonal band has developed that links the two regions of high effective stress.

The next three figures show the strain and stress distributions at the midsection, $z = 0$. As in [12], these are not actually the distributions at $z = 0$ but are the stresses and strains associated with the nodes on the line BC of Fig. 3.

The strain distributions are shown in Fig. 8, at two stages of compression. It can be seen in this figure that the strain components reach their peak values on the axis of the bar

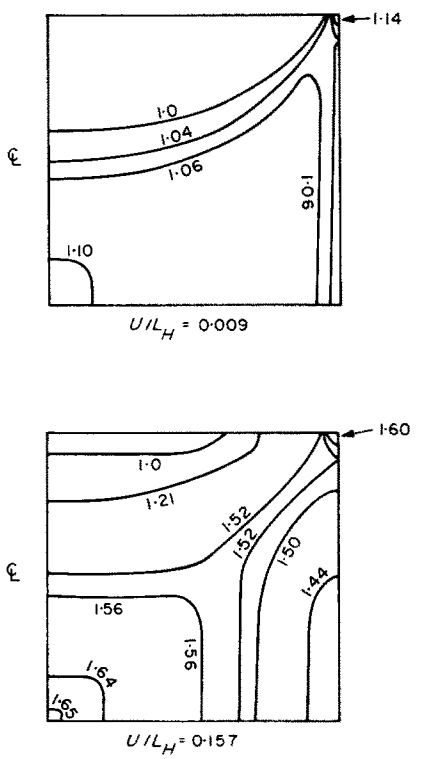

FIG. 7. Contours of effective stress in original configuration for two stages of compression ($n = 8$, $\varepsilon_y = 0{\cdot}0072$, $\nu = \frac{1}{3}$, $L_H/R_0 = 1$).

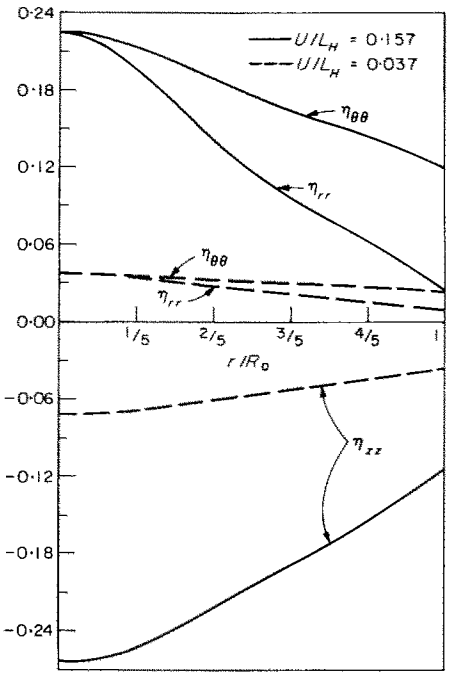

FIG. 8. Strain distributions at midsection at two stages of compression ($n = 8$, $\varepsilon_y = 0{\cdot}0072$, $\nu = \frac{1}{3}$, $L_H/R_0 = 1$).

and that these peaks become accentuated as deformation proceeds. Also, note that η_{rr} and $\eta_{\theta\theta}$ are not equal except near $r = 0$.

Finally, Figs. 9 and 10, respectively, display the stress distributions at the midsection for $U/L_H = 0{\cdot}037$ and $U/L_H = 0{\cdot}157$. Surprisingly, each stress component reaches a local minimum slightly off the axis of the column. This minimum is sharper in the latter stages of compression. However, the effective stress does reach its maximum at $r = 0$. Two

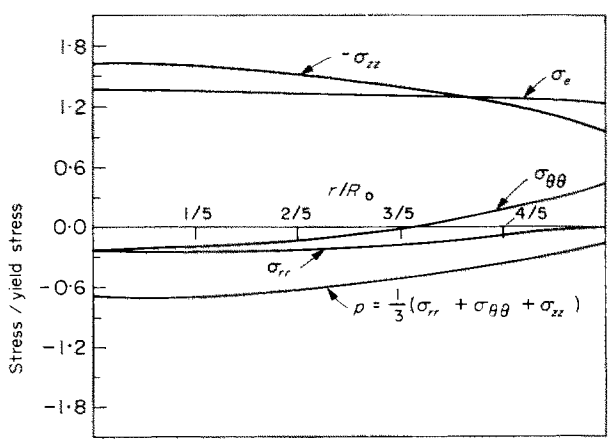

FIG. 9. Stress distribution at midsection at $U/L_H = 0{\cdot}037$ ($n = 8$, $\varepsilon_y = 0{\cdot}0072$, $\nu = \frac{1}{3}$, $L_H/R_0 = 1$).

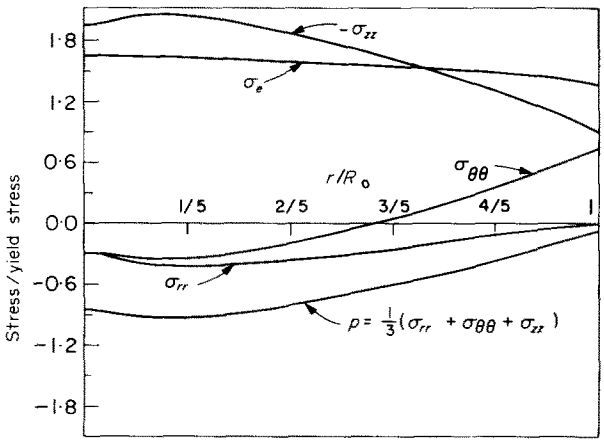

FIG. 10. Stress distribution at midsection at $U/L_H = 0{\cdot}157$ ($n = 8$, $\varepsilon_y = 0{\cdot}0072$, $\nu = \frac{1}{3}$, $L_H/R_0 = 1$).

noteworthy features of the stress distributions are; a positive hoop stress, $\sigma_{\theta\theta}$, at the lateral surface and the fact that the effective stress obtained here is not uniform across the mid-section.

Also shown in Figs. 9 and 10 is the triaxial tension given by

$$p = \tfrac{1}{3}(\sigma_{rr} + \sigma_{\theta\theta} + \sigma_{zz}).$$

This quantity is of particular importance since it is currently thought, see [15], that an important mechanism of ductile fracture is the growth and coalescence of voids driven by a positive triaxial tension. Here, p is found to be least negative at $r = R_0$, that is, at the lateral surface. Furthermore, the triaxial tension at $r = R_0$ becomes less negative as deformation proceeds. Unfortunately, the present calculation could not be continued far enough for p at the lateral surface to become positive. However the experiments of Kuhn and Lee [16], which show voids developing on the surface of a circular cylindrical compression specimen, lend support to the contention that the triaxial tension does eventually become positive at $r = R_0$.

Acknowledgement—This work was partially supported by NSF Grant GP 22796.

REFERENCES

[1] F. R. SHANLEY, Inelastic column theory. *J. Aero Sci.* **14**, 261 (1947).
[2] R. HILL and M. J. SEWELL, A general theory of inelastic column failure—I. *J. Mech. Phys. Solids* **8**, 105 (1960).
[3] R. HILL, A general theory of uniqueness and stability in elastic-plastic solids. *J. Mech. Phys. Solids* **6**, 236 (1958).
[4] R. HILL, Bifurcation and uniqueness in non-linear mechanics of continua. *Problems of Continuum Mechanics*, p. 155, Society for Industrial and Applied Mathematics (1961).
[5] S. Y. CHENG, S. T. ARIARATNAM and R. N. DUBEY, Axisymmetric bifurcation in an elastic-plastic cylinder under axial load and lateral hydrostatic pressure. *Q. appl. Math.* 29, 41 (1971).
[6] J. B. NEWMAN, Geometric instabilities in isotropic plastic solids under increasing uniaxial compression. *J. appl. Mech.* **39**, 431 (1972).
[7] A. E. GREEN and W. ZERNA, *Theoretical Elasticity*. Oxford University Press, Oxford (1968).

[8] B. BUDIANSKY, Remarks on theories of solid and structural mechanics. *Problems of Hydrodynamics and Continuum Mechanics*, p. 77. Society for Industrial and Applied Mathematics (1969).
[9] J. W. HUTCHINSON, Post-Bifurcation Behavior in the Plastic Range. Harvard University Report SM-54 (1971).
[10] B. BUDIANSKY, To be published.
[11] W. CHEN, Necking of a bar. *Int. J. Solids Struct.* **7**, 685 (1971).
[12] A. NEEDLEMAN, A numerical study of necking in circular cylindrical bars. *J. Mech. Phys. Solids* **20**, 111 (1972).
[13] C. E. PHILLIPS, Recent advances in time-independent plasticity at the national engineering laboratory. *Recent Progress in Applied Mechanics* (The Folke Odqvist Volume) p. 415. Almqvist and Wiksell, Stockholm (1967).
[14] H. VAUGHAN, Axisymmetric and asymmetric instabilities in elastic solid cylinders under finite axial strain. *Zamp* **22**, 865 (1971).
[15] J. I. BLUHM and R. J. MORRISSEY, Fracture in a tensile specimen. *Proceedings of the 1st International Conference on Fracture* (Sendai), p. 1739. Japanese Society for Strength and Fracture of Metals (1966).
[16] H. A. KUHN and P. W. LEE, Strain instability and fracture at the surface of upset cylinders. *Met. Trans.* **2**, 3197 (1971).

(*Received* 5 *October* 1972; *revised* 16 *February* 1973)

Абстракт—Даются два разных способа формулировки краевой задачи для круглой, упруго-пластической колонны, под влиянием одноосного сжатия. Во первом. предполагается концы колонны являются прикрепленными к жестким плитам, тогда как в другом они свободны от сдвига. Для этого последнего краевого условия, получается одно решение, которое соответствует состоянию однородного, одноосного напряжения для всех значений приложенного сжатия. Методом конечного элемента исследуется класс форм бифуркации для этого решения. В качестве специальных случаев, этот класс заключает продольныи изгиб стойки в смысле Эйлера и осесимметрическое выпучивание. Оказывается затем, что единственной формой бифуркации, которую можно вероятно реализовать в упруго-пластических материалах, рассматриваемого здесь класса [для реальных значений параметров материала], является продольнвй изгиб стержня в смысле Эйлера. Подсчияывается, также, полная история деформации для короткой колонны, прикрепленной к жестким плитам. Для этого случая, ограничивается внимание к осесимметрическим деформациям. Полученные результаты приводят полную кривую нагрузка—деформация, для колонны, прикрепленной к жестлим плитам и распределение напряжений и деформаций для среднего сечения.